

Long-term stability of sodium caseinate-stabilized nanoemulsions

Manispuritha Yerramilli¹ · Supratim Ghosh¹ 

Revised: 8 September 2016 / Accepted: 9 December 2016 / Published online: 11 January 2017
© Association of Food Scientists & Technologists (India) 2017

Abstract Oil-in-water (5 wt%) nanoemulsions were prepared with different concentration (2.5–10 wt%) of sodium caseinate as a sole emulsifier and their long-term storage stability was investigated for 6 months. Previous studies associated with sodium caseinate looked only into nanoemulsion formation; hence the challenges with long-term stability were not addressed. All nanoemulsions displayed an average droplet size <200 nm, which remained unchanged over 6 months. However, all of them displayed rapid creaming due to unabsorbed protein induced depletion flocculation, whose extent increased with protein concentration, although the cream layer formed was weak and re-dispersible upon gentle mixing. Microstructural analysis of the cream layer showed compaction of flocculated nanodroplet network with time leaving the aqueous phase out. Calculation of depletion interaction energy showed an increase in inter-droplet attraction with protein concentration and decrease with a reduction in droplet size, making the nanoemulsions more resistant to flocculation than conventional emulsions. This work aids in understanding the dependence of protein concentration on long-term stability of sodium caseinate-stabilized nanoemulsions.

Keywords Sodium caseinate · Nanoemulsion · Depletion flocculation · Long-term stability · Creaming · Photocentrifuge

Introduction

Nanoemulsions (NEs) are emulsions where the majority of the dispersed droplets fall within the nanoscale range. It has been proposed that average droplet radii of NEs should be <100 nm (McClements 2012), however, others considered the upper range to be 200 nm or at times even higher (Fernandez et al. 2004; Gutiérrez et al. 2008). For example, Sanguansri and Augustin defined nanoemulsions for droplet diameter ranging from 50 to 1000 nm. Due to their small droplet sizes, NEs have several advantages compared to conventional emulsions. They were found to have higher stability to droplet aggregation and gravitational separation, high optical clarity when the droplet size and volume fraction is below a critical level (McClements 2011) and display potential to modulate product texture (Erramreddy and Ghosh 2014). Oil-in-water (O/W) NEs are being utilized in food applications to encapsulate and deliver poorly water-soluble active ingredients (e.g., vitamins, antioxidants, nutraceuticals, preservatives and flavors) (Rao and McClements 2012). In vitro studies have shown that the bioavailability of these encapsulated components was significantly higher in NEs than conventional emulsions due to the high surface-to-volume ratio of nanodroplets (Acosta 2009; Ahmed et al. 2012). Recently, Paul et al. (2014) studied the efficacy of bitter gourd seed oil (containing ~50% α -eleostearic acid) NE in improving the bioavailability of conjugated linolenic acid from rat gastrointestinal tract. The NEs were prepared using a low energy phase inversion process where span 80 added oil phase was mixed with Tween 20 added aqueous phase followed by high-energy processing to lower the average droplet diameter below 100 nm and remained stable throughout the 12 weeks study period. It was found that the diet

✉ Supratim Ghosh
supratim.ghosh@usask.ca

¹ Department of Food and Bioproduct Sciences, University of Saskatchewan, Saskatoon, SK, Canada

supplementation with nanoemulsion exhibited maximum efficiency in countering oxidative stress in different organs compared to the conventional emulsions with large droplet size (Paul et al. 2014). These advantages of NEs not only provide strong evidence of their improved applications in food and beverages, but also in chemical, agriculture and pharmaceutical industries where higher release of chemicals, pesticides or drug molecules may lead to better utilization and cost-effectiveness (Ahmed et al. 2012; Rao and McClements 2012).

To create extremely small droplets of O/W NEs, a lot of water-soluble emulsifiers are required. An essential criterion for the selection of emulsifiers is their ability to lower interfacial tension so that nano-size droplets can be created, and move faster towards freshly created bare nanodroplet surfaces during homogenization. Many small molecule emulsifiers, including sodium dodecyl sulfate (SDS), Tweens, etc. (Hashtjin and Abbasi 2015; Galooyak and Dabir 2015), can meet both of these criteria, but large quantities of these emulsifiers in food and drug is not preferred due to toxicological concerns (He et al. 2011). In this respect, food proteins are ideal candidate to stabilize NEs as they do not raise toxicological concerns and improve consumer acceptance (Karaca et al. 2011), although their ability to lower interfacial tension and movement towards bare interfaces during homogenization are significantly lower than small molecule emulsifiers. Nevertheless, if a NE can be formed with proteins, they tend to provide better long-term stability due to the formation of a thick viscoelastic membrane on droplet surface that acts as a protective coating (Walstra 2002).

Among the various food proteins, those isolated from bovine milk (casein and whey proteins) are widely used as emulsifying agents in a variety of food products including beverages, ice creams, sports supplements, infant formula and coffee creamer (McClements 2005). The protein casein consists of four fractions: α_{s1} (~44 wt%), α_{s2} (~11 wt%), β (~32 wt%), and κ (~11 wt%) and it has well-defined hydrophobic and hydrophilic regions that help in rapid adsorption at the oil–water interface (Aleandri et al. 1968). The sodium salt of casein, popularly referred to as sodium caseinate (SC), is essentially a soluble mixture of all four fractions of caseins (Radford and Dickinson 2004). High solubility of SC has been exploited widely for its use as an emulsifier for conventional emulsions and also NEs (Hunt and Dalgleish 1994; Lee and Norton 2013; Qian and McClements 2011; Zeeb et al. 2014; Zhao et al. 2015). Reports of use of calcium caseinate in the development of NE has also been made where the authors form a conjugate of calcium caseinate with sodium alginate to stabilize O/W NE with an average droplet diameter in the range 200–300 nm (SenGupta and Ghosh 2015).

It has also been observed that the stability of SC-stabilized emulsions and NEs was largely influenced by the presence of un-adsorbed free proteins in the continuous phase (as sub micelles in the order of 15–20 nm) (Dickinson and Golding 1997) leading to depletion flocculation (Aronson 1989). Extensive attempts have been made on SC-stabilized conventional emulsions in order to prevent depletion flocculation by keeping protein concentration level below a critical limit or by including other components in the system that curbed the depletion effects associated with SC (Liang et al. 2014; Zhao et al. 2015). In this regard, whey protein isolate (Hunt and Dalgleish 1994), polysaccharides (maltodextrin or xanthan gum) (Liang et al. 2014), various alcohols (ethanol, 1-propanol, 1-butanol) (Zeeb et al. 2014) and flaxseed protein (Zhao et al. 2015) have been used. However, preparation of NEs stabilized with SC alone as an emulsifier has not been explored in details. Most of the studies associated with SC looked into NE formation by measuring droplet size and did not include any long-term stability study. Hence, the issues of depletion flocculation were not addressed (Lee and Norton 2013; Qian and McClements 2011). The objective of the current research is to investigate long-term stability of SC-stabilized O/W NEs against depletion flocculation. All NEs were prepared with 5 wt% canola oil with different concentrations of SC, and their storage stability was studied for 6 months using droplet size, microstructure, gravitational and accelerated stability analysis.

Materials and methods

Materials

Canola oil was purchased from local grocery store. Milli-QTM water (Millipore Corporation, MA, USA) was used for the preparation of continuous aqueous phase. Casein sodium salt from bovine milk (SC) was purchased from Sigma Aldrich (Oakville, ON, Canada). SDS was purchased from Fisher Scientific (Nepean, ON, Canada). All the other chemicals were purchased from Sigma Aldrich (Oakville, ON, Canada).

Preparation of aqueous phase

A 10 wt% protein stock solution was prepared by dispersing SC in Milli-QTM water and left overnight stirring on a bench top magnetic stirrer (VWR international, AB, Canada) at room temperature. To this, 0.01 wt% sodium azide was added to avoid microbial contamination. This stock solution was serially diluted to obtain solutions

containing 2.5, 5 and 7.5 wt% SC. pH of the freshly prepared protein solutions were ranged from 6.8 to 7.2.

Preparation of nanoemulsions

The oil phase (5 wt% canola oil) and aqueous phase (95 wt%) containing the different amount of SC were coarsely mixed on a benchtop magnetic stirrer. An oil-in-water coarse emulsions was prepared from this pre-mix using a rotor/stator mixer (Polytron, Brinkmann instruments, ON, Canada) for 2 min at 20,000 rpm which was then passed through a high-pressure homogenizer (Emulsiflex-C3, Avestin Inc., Ottawa, ON, Canada) at a pressure of 20,000 psi (137.9 MPa) for 6 cycles in order to develop NE. Emulsification was done at room temperature although the final temperature of the NEs rose to $\sim 40^\circ\text{C}$. The pH and conductivity of all NEs ranged between 6.8 and 7.1 and 10–20 $\mu\text{S}/\text{cm}$, respectively.

Emulsion storage stability

All freshly prepared NEs were stored in 40 ml clear glass vials (VWR international, AB, Canada) for long-term stability analysis (6 months) through visual observation and creaming index measurement. For all the other experiments NEs were stored in two separate 50 ml clear polypropylene centrifuge tubes (VWR international, AB, Canada), one exclusively for microscopy (to understand the microstructure of the cream layer and the serum layer without disturbing the sample) and the other for the rest of the experiments (droplet size, bulk microscopy and accelerated stability analysis). All sample vials were stored in a refrigerator at 4°C .

Droplet size distribution

The droplet size distribution of the NEs was determined using a static laser diffraction particle size analyzer (Mastersizer 2000, Malvern Instruments, Montreal, QC, Canada) in accordance to the standard ISO 13,320 with a relative refractive index of the dispersed to continuous phases of 1.465. Drops of NE was added to the sample dispersion unit until the obscuration index reached about 15% and the droplet size distribution and the surface mean diameter (d_{32}) was measured. As the NEs displayed creaming, a uniform sample was drawn by gently mixing them before the experiment.

Creaming index

Creaming of NEs was visually observed and recorded using a digital camera from the samples stored in transparent glass vials and quantified by calculating creaming index

(CI), defined as the ratio of the height of the bottom serum layer (H_S) to the total height of the emulsion (H_E) (McClements 2007). A creaming index of 1 signifies stable, non-creamed emulsion and the values decrease with increase in creaming.

Microscopy

Confocal microscopy

The structure of the freshly prepared NEs was also analyzed by confocal laser scanning microscope (CLSM). For this, emulsions were separately prepared using 0.01 wt% Nile red dye (Sigma Aldrich, Oakville, ON, Canada) in the oil phase. Samples were examined with a Nikon C2 CLSM microscope (Nikon, Mississauga, ON, Canada) using a 543 nm laser using a $63\times$ Plan Apo VC (N.A. 1.4, Nikon) oil immersion objective lens. The sample tubes were gently mixed to re-disperse the cream layer before taking it for microscopy.

Optical microscopy

An optical microscope (Eclips E400, Nikon Mississauga, ON, Canada) was used to capture microstructure of the cream. All experiments were carried out at magnifications of $100\times$ and $400\times$. Samples from cream and serum phases were drawn without disturbing the layers. A drop of the sample was placed on a microscope slide (Fisher Scientific, Nepean, ON, Canada) covered with a coverslip (VWR International, AB, Canada) and observed under the microscope.

Centrifugal separation analysis

The multi-sample photocentrifuge—LUMiSizer LS650 (LUM GmbH, Berlin, Germany) was used to understand the accelerated storage stability of the NEs. This equipment employs the STEP (Space and Time resolved Extinction Profiles) technology, which measures the intensity of transmitted light as a function of time and position over the entire sample length in a cuvette during centrifugation (Lerche 2002). It displays data in the form of transmission profiles of emulsions as a function of sample height in the cuvette. 350 μl of sample was placed in rectangular polycarbonate cuvettes (2×8 mm) (LUM GmbH, Berlin, Germany) and centrifuged at a speed of 4000 rpm ($2266\times g$) at 25°C to capture 1000 transmission profiles at an interval of 60 s (total run time was 16 h 40 min) using a laser wavelength of 865 nm. The progression of the transmission profiles contained information on the kinetic stability of the emulsions using SEPView software v 4.1 (LUM GmbH, Berlin, Germany). The instability or

separation index, a factor calculated by the software and whose derivation and calculations can be found elsewhere in detail (Detloff et al. 2013), was used to compare the stability of NEs. Briefly, instability index quantifies the clarification in transmission based on particle size and separation at a given time in the presence of accelerated gravitational force, divided by the maximum clarification possible. The clarification is due to increase in transmission or decrease in droplet concentration due to movement of nanodroplets towards the cream layer. It is a dimensionless number between 0 and 1, where 0 indicates no separation or no change in NEs' transmission and hence highest stability, and 1 represents complete segregation of phases and hence lowest stability under the centrifugal field. Comparing instability indices of NEs under accelerated gravitational field ultimately aids in a quick comparison of their shelf-life instead of waiting long-time at earth gravitation.

Statistics

Samples were prepared, and experiments were performed with at least three replicates. Student's *T* test for independent samples was applied to determine the statistical significance at a 95% confidence level using SPSS software (SPSS Inc., ver. 22, 2013, Chicago, IL).

Results and discussion

Droplet size distribution

Droplet size distributions of the NEs are reported in Fig. 1a. All NEs have a monomodal distribution ranging from 30 nm to <1 μm . Similar droplet size distribution was also observed by many researchers for sodium caseinate and whey protein isolate-stabilized nanoemulsions (Qian and McClements 2011; Lee and McClements 2010). To understand the change in droplet size distributions as a function of time, comparisons were made with freshly prepared [Fig. 1a (I)] and 24 weeks (6 months) old samples [Fig. 1a (II)]. No change in the distribution of these NEs was visible over the period of 6 months. It should be noted that the effect of depletion flocculation was not seen in the droplet size distribution as during the light scattering measurements the samples were diluted to a great extent (few drops added to the reservoir of 150 ml in the instrument) thereby the concentration effect of excess SC submicelles were cancelled. Absence of flocculation was also confirmed by measuring the droplet size after gently mixing the NEs with 0.1 wt% SDS solution (1:5 ratio) where no change in droplet size distribution was observed (data not shown). The surface average droplet diameters (d_{32}) of all NEs were plotted as a function of time in Fig. 1b. The

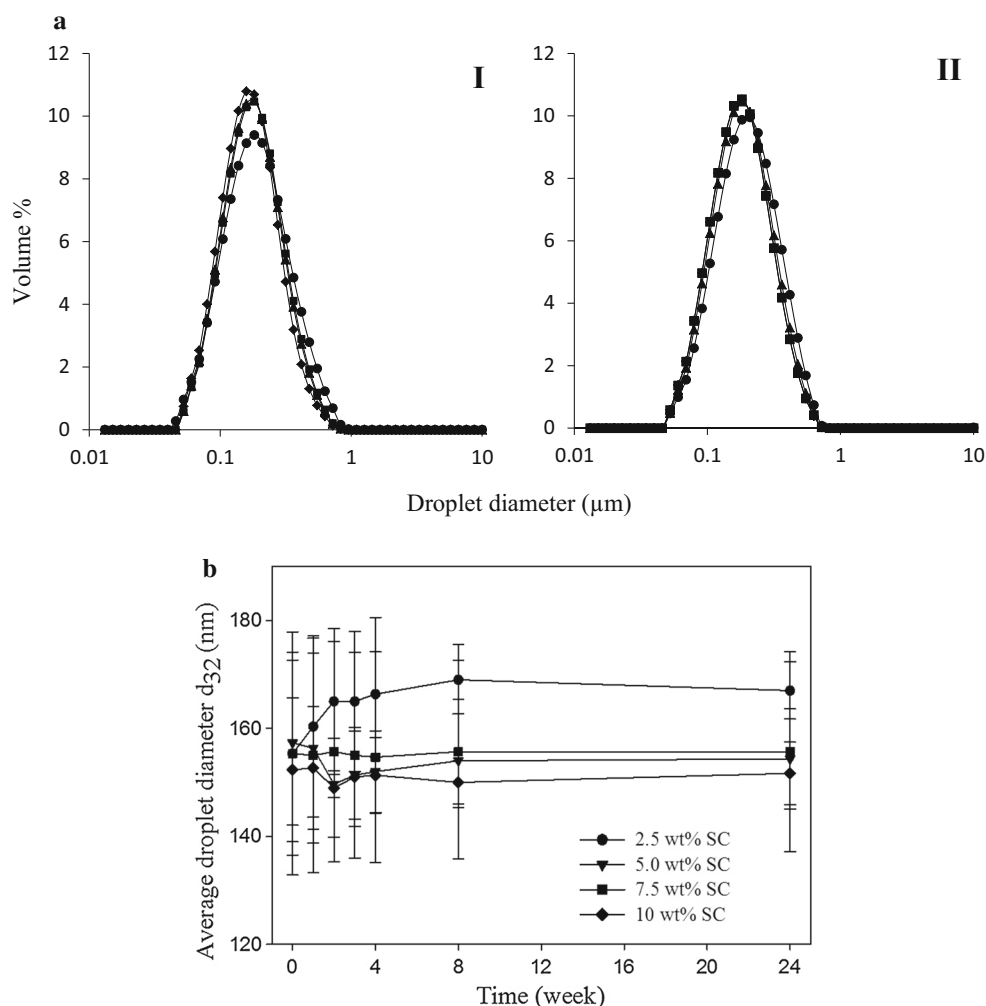
d_{32} values of all NEs were in the range of 155–170 nm, which falls in the range below 200 nm definition of NEs proposed by McClements (2012). Moreover, the NEs in the present case did not show any significant change in their d_{32} values over a period of 24 weeks ($p > 0.05$). Among the different NEs, only the average d_{32} values of 2.5 wt% samples were higher than all other NEs although not statistically significant ($p > 0.05$).

Visual observation of the nanoemulsions

Visual observation of the NEs was recorded to understand the extent of creaming and its influence on the overall stability of the NEs. The inset of Fig. 2 shows images of undisturbed NEs in vials after 24 weeks of storage. Although the NEs remain stable (no change in average droplets size) over a period of 6 months, they showed distinct cream layer formation, which increased with protein concentration. This type of creaming in SC-stabilized emulsions has previously been observed when excess protein concentration in the continuous phase induced depletion flocculation (Dickinson and Golding 1997; Dickinson et al. 1997; Liang et al. 2014). We, however, noticed that the creaming is weak and reversible and can be avoided by regular gentle mixing of the NEs. In fact, for the samples used for droplet size and bulk microscopy, hence gently mixed on a regular basis, we did not observe any creaming (data not shown). Nevertheless, for conventional emulsions with larger droplets and higher oil concentration, depletion flocculation could lead to stable droplet network, which upon compaction and rearrangement expulse aqueous phase as bottom serum layer. This type of serum layer separation was measured by Dickinson and co-workers using ultrasonic scanning technique (Dickinson and Golding 1997; Dickinson et al. 1997). Liang et al. (2014) investigated creaming of 30 wt% O/W emulsions stabilized with different concentration of SC ($d_{32} = 0.7 \mu\text{m}$) and also reported that the depletion flocculation of large droplets formed a network of clusters which led to the creaming of the whole emulsion phase leaving a clear serum layer at the bottom. The advantage of NEs is that they are inherently very stable against flocculation due to their small droplet size (Tadros et al. 2004). Therefore, although depletion interaction due to unadsorbed SC in the continuous phase is present, nanodroplets' inherent stability against flocculation made them easily re-dispersable by gentle mixing. Also, the fact that we had only 5 wt% oil played a significant role in the inability to form strong clusters of flocculated droplets.

It should be noted that the SC-stabilized nanoemulsions reported here are opaque and not transparent or translucent as reported in some literature (Lee and McClements, 2010; Xue and Zhong, 2014). However, for a nanoemulsion to be transparent or translucent, its droplet size distribution, oil

Fig. 1 Droplet size distribution (a) and surface average mean droplet diameter (d_{32}) (b) of 5 wt% canola oil-in water nanoemulsions stabilized by various concentrations of sodium caseinate for (I) freshly prepared and (II) 24 weeks old samples (a) and as a function of time (b). Nanoemulsions prepared with protein concentrations of 2.5 wt% (circle), 5 wt% (triangle), 7.5 wt% (square), 10 wt% (diamond) are compared



volume fraction and refractive index contrast between the two phases should be below a critical level. Using Mie theory McClements proposed that for a monodispersed emulsion to be transparent, its average droplet diameter should be <40 nm, while for a polydisperse emulsion it should be less than about 20–30 nm. Wooster et al. (2008) developed 15 wt% peanut oil-in-water nanoemulsions using SDS and PEG as emulsifiers and showed that transparency appeared when the entire droplet size distribution was below 80 nm and the average droplet diameter was below 40 nm. It was also proposed that reduction in refractive index difference between the oil and aqueous phase may also improve transparency of nanoemulsions. Turbidity or opaqueness of nanoemulsions can also increase with oil concentration (Lee and McClements 2010; McClements, 2011). Xue and Zhong (2014) prepared thyme oil nanoemulsions with SC and found that 5% w/v SC was able to deliver a transparent or translucent nanoemulsions only if the oil fraction is less than or equal to 1% w/v where the average hydrodynamic diameter was ≤ 105 nm. At 2% w/v thyme oil the average hydrodynamic diameter was ~ 180 nm and the

nanoemulsion transformed into an opaque system. In the present case, the SC-stabilized nanoemulsions contained 5 wt% oil and the average droplet diameter ranged from 130 to 180 nm, with the size distribution extends to almost 900 nm, hence they are not transparent or translucent in appearance.

Determination of creaming index (CI)

In order to quantify creaming in undisturbed NEs, the height of the cream layer was measured, and average creaming indices were plotted as a function of time (Fig. 2). It can be observed that after a week of preparation, all NEs showed creaming as CI decreased from its initial value of 1. The formation of the cream layer from freshly made NEs was very rapid, and a discernable cream layer was visible within few hours after preparation. After 1 week the drop in CI, hence extent of creaming increased with protein concentration. However, after this initial drop for the NEs with 2.5 and 5 wt% SC the change in CI with time was not significant for the rest of the 24 weeks of storage ($p > 0.05$), while for 7.5

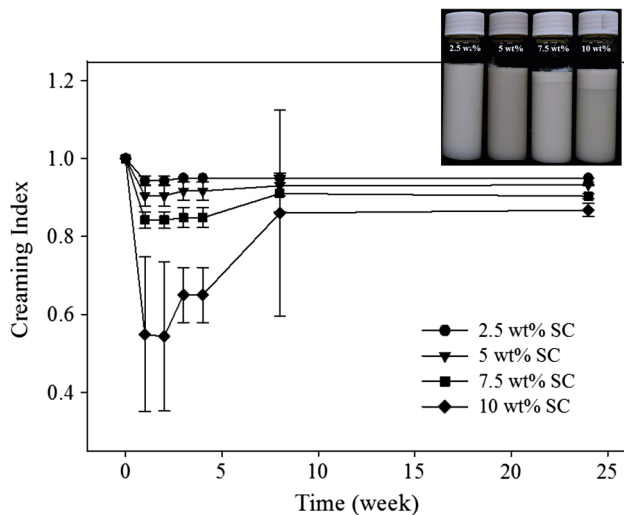


Fig. 2 Change in creaming index of oil-in-water nanoemulsions stabilized by various concentrations of sodium caseinate as a function of storage time. *Inset* shows visual observation of the nanoemulsions in glass vials after 6 months (24 weeks) of storage. Different aqueous phase protein concentrations: 2.5 wt% (circle), 5 wt% (triangle), 7.5 wt% (square), 10 wt% (diamond)

and 10 wt% NEs, a significant change in CI was observed ($p < 0.05$). For 7.5 wt% NE, the CI remained unchanged from 1 to 4 weeks, thereafter increased (due to compaction of the cream layer) until 8 weeks and remained unchanged for the rest of the 6 months. For 10 wt% SC NEs similar behaviour was observed, except that the compaction of the cream layer began after 2 weeks of storage. From the CI data it is apparent that the full extent of creaming takes about a week to form, thereafter compaction of cream layer begins which stopped when no more oil droplets and proteins can be packed in the top cream layer. Similar behavior of compaction/compression of cream layer was observed in emulsions with excess unadsorbed polymers in the continuous phase (Fillery-Travis et al. 1993; Newling et al. 1997). It was proposed that the droplets in the cream layer underwent compression/compaction under the influence of gravity by gradually re-arranging with time leaving the serum layer squeezed out (Newling et al. 1997). The weak attractive force among the droplets in the cream later also allowed them to re-arrange under the influence of gravity (McClements 2007). To understand the changes brought about by the compaction of the cream layer, we also looked into the evolving microstructure of these systems.

Microstructure

Figure 3 shows the confocal micrographs of the NEs taken one day after preparation. All NEs contained numerous small oil droplets in a flocculated state. The extent of flocculation appeared more with the increase in

protein concentration, which is in accordance with higher cream layer thickness seen during visual observation (Fig. 2). The extremely small droplet size of the NEs made it difficult to capture clear images of droplet flocculation with the present set up of the confocal microscope. In order to clearly visualize the floc structure, one image of 2.5 wt% SC NEs was captured with 5 times digital zoom of the 63 X objective lens (Fig. 3e). It can be observed that nearly monodisperse nanodroplets are flocculated forming large clusters. Numerous small clusters of droplets can also be seen in the background. The microstructure of the NE is distinctly different from conventional emulsions with large droplet sizes and higher oil volume fractions seen by other researchers. For

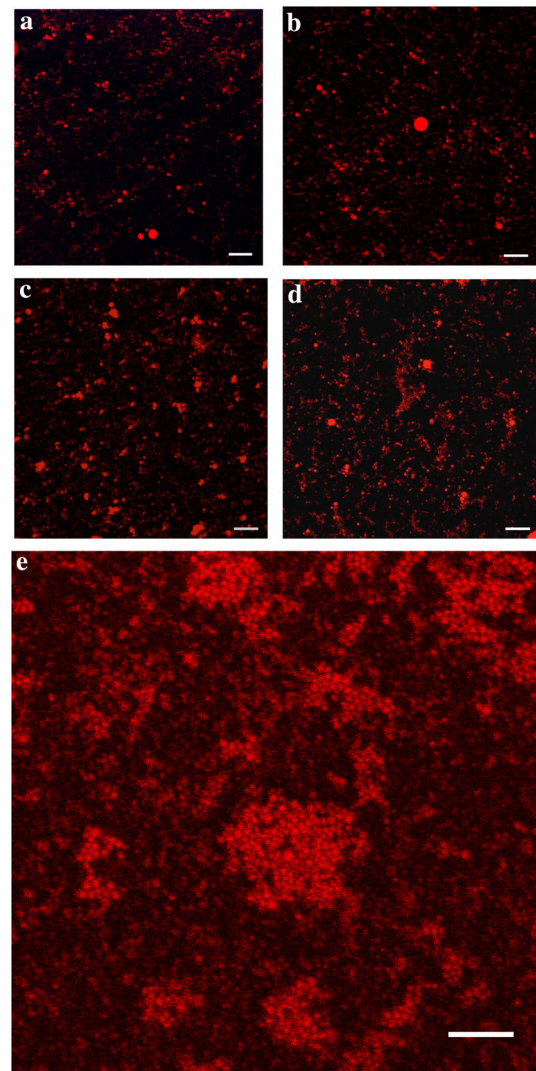


Fig. 3 Confocal micrographs of 5 wt% canola oil-in-water nanoemulsions stabilized by various concentrations of sodium caseinate **a** 2.5 wt%, **b** 5 wt%, **c** 7.5 wt% and **d** 10 wt% (scale bar 20 μm). The nanodroplet flocs are clearly visible in **(e)** which was captured by 5 times digital zooming on a 2.5 wt% sodium caseinate-stabilized nanoemulsion sample (scale bar 5 μm)

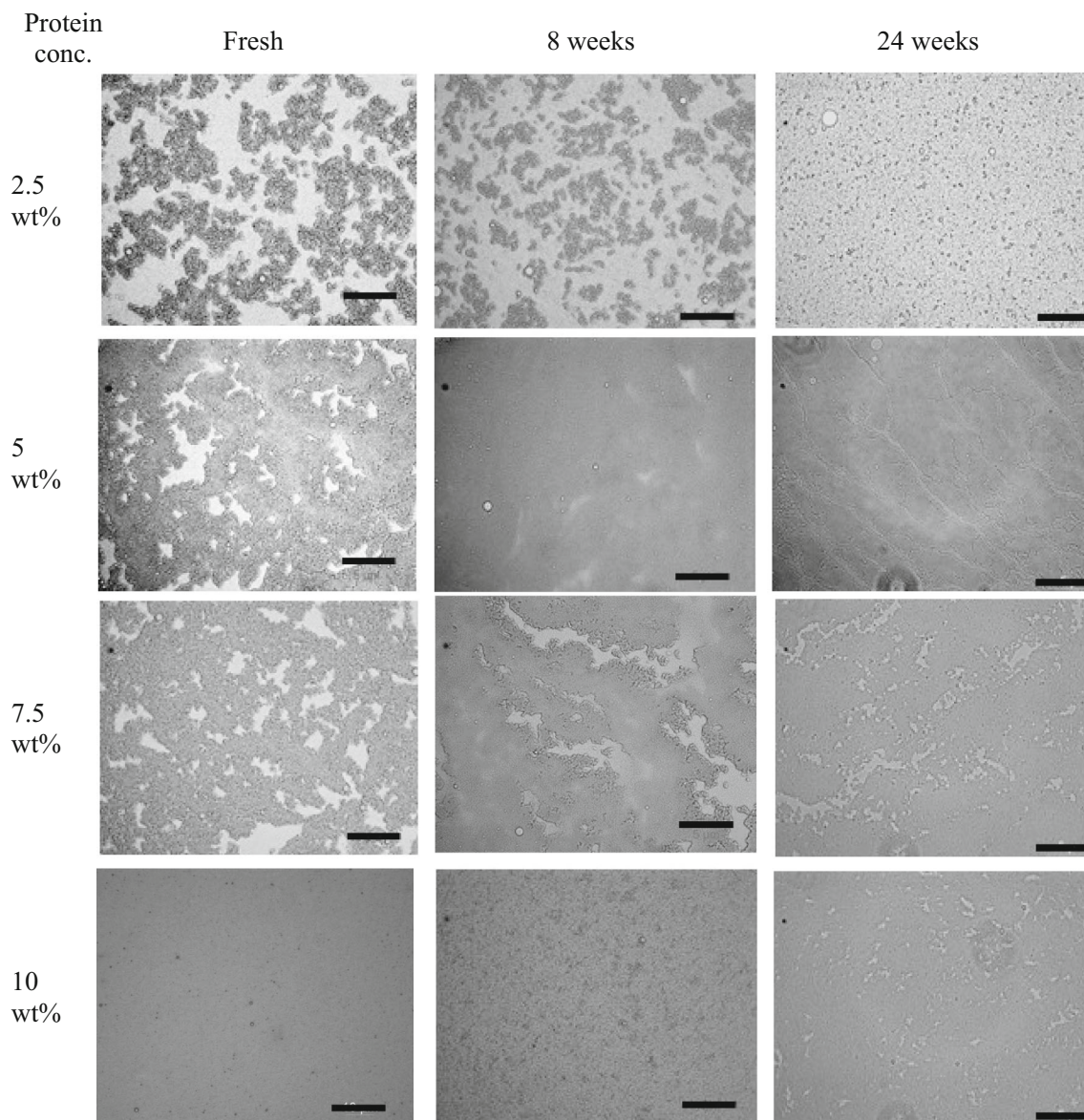


Fig. 4 Optical micrographs of the cream layer from 5 wt% canola oil-in-water nanoemulsions stabilized by sodium caseinate at various concentrations on the day of preparation and after 8 and 24 weeks of

storage. A working magnification of 400 \times was used. Scale bar represents 5 μ m

example, Dickinson and co-workers (Dickinson and Golding 1997), in their pioneer work on creaming and flocculation of SC-stabilized O/W emulsions, found flocculated droplet network throughout the emulsion micrographs. For their microscopy work, the authors used 10 vol% O/W emulsions stabilized with various concentration of SC. For these emulsions, a distinct cream layer was observed when SC concentration reached 2.4 wt%. At 3 wt%, highly flocculated droplet clusters formed a network throughout the emulsion which prevented further creaming. Liang et al. (2014) used a confocal microscope to record microstructure of SC-stabilized conventional

emulsions containing 30 wt% oil. The authors also observed extensive flocculation of oil droplets throughout the emulsions. In the present case, only 5 wt% oil was used which was not enough to form a network of droplet clusters (Fig. 3e). Also, as discussed in the following section, NEs are more stable against depletion flocculation compared to conventional emulsions, which manifested as less aggregated droplets visible in the confocal micrographs.

However, a different observation of flocculated nanodroplet structure was obtained when the undisturbed cream layer of the NEs were recorded as a function of time

(Fig. 4). It can be seen that in 2.5 wt% SC NE cream, the droplet aggregates formed clusters, however, the clusters could not form a network. With the increase in protein concentration (5–10 wt% SC), the clusters of droplets formed an extensive network. As a function of time and at higher protein concentration as the cream layer compacted, the entire micrographs became filled with the nanodroplet network. The continuous aqueous phase expelled from the network (no gap can be seen) leaving a solid-like state made up mostly of packed nanodroplets. Packing of droplets was more evident after 6 months of storage compared to 8 weeks. The 2.5 wt% SC NEs, however, behave differently after 6 months of storage. As discussed below, due to very weak depletion interaction at 2.5 wt% SC, a very fine cream layer was formed after 6 months (Fig. 2) and its micrograph with much less cluster formation appeared different from the rest of the NEs.

Centrifugal separation analysis

The centrifugal separation analysis using a photocentrifuge is a novel means of comparing emulsion stability in an accelerated gravitational field. We have used this analytical technique as a supplemental method to the conventional creaming index measurement. Figure 5 shows the change of instability index with time for all NEs. Instability index aided ranking of our samples in terms of stability against phase separation. It can be observed that instability index decreased with increase in protein concentration, indicating the 10 wt% SC NE was the most stable one. Statistically, 2.5, 5 and 7.5 wt% SC NEs are not significantly different in terms of instability index ($p > 0.05$) which was indeed the case for CI measurement under 6 months storage (Fig. 2). From Fig. 5 it can also be seen that the 10 wt% SC NE was significantly more stable than 2.5 and 5 wt% ($p < 0.05$), while no significant difference was observed with 7.5 wt% SC NE ($p > 0.05$). As a function of time, no significant difference in instability indices was observed for all NEs ($p > 0.05$), although for 10 wt% NE the values of instability indices increased after 6 months of storage (from 0.65 for fresh NE to 0.82 after 6 months). The results for NE stability under accelerated gravitation appears to contradict what we have seen in creaming behavior of undisturbed sample under gravity (Fig. 2), where extent of creaming increased (stability decreased) with increase in protein concentration due to depletion flocculation. This could be due to the oversaturation of the instrument detector at high protein concentration where a large number of casein submicelles and droplet flocs prevented clear detection of droplet movement and hence the NEs appeared more stable. This showed a limitation of the centrifugal

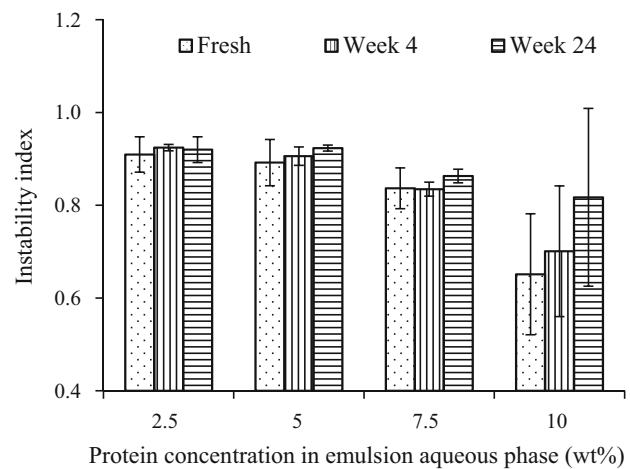


Fig. 5 Instability index calculated from centrifugal separation analysis transmission profiles of the nanoemulsions prepared with various concentrations of sodium caseinate for freshly prepared, 4 and 24 weeks old samples

separation method, and may be overcome by suitable dilution of the system.

Calculation of depletion interaction energy

Dickinson and co-workers have proposed depletion flocculation as a possible mechanism of destabilization in SC-stabilized emulsions (Dickinson and Golding 1997; Dickinson et al. 1997). Attempts have also been made by the researchers to bring in stronger evidence to prove Dickinson hypothesis (Liang et al. 2014). Three different stages of emulsion stability have commonly been observed: the regime with no creaming and droplet flocculation was observed at a SC concentration sufficient for nearly saturation coverage of the droplets. At a lower protein concentration than this there were insufficient proteins for complete coverage of the droplet surface, and hence, protein molecules adsorbed on one droplet may be shared with other droplets leading to emulsion destabilization due to bridging flocculation. On the other hand, the presence of excess unabsorbed protein resulted in reversible droplet flocculation due to depletion interaction, where saturation coverage of droplets by proteins was able to prevent any further coalescence. In this case depletion interaction energy (ΔG_{dep}) can be calculated from Eq. 1:

$$\Delta G_{dep} = -VP_{osm} \quad (1)$$

where, V is the volume of the emulsifier depleted layer between two approaching droplets and P_{osm} is the osmotic pressure created by the presence of excess proteins in the emulsion continuous phase (Dickinson and Golding 1997; McClements 1994). Here we considered maximum

depletion interaction when the droplet surfaces touch in which case the volume of the depleted layer could be estimated by

$$V = 2\pi r_m^2 \left(r_d + \frac{2r_m}{3} \right) \quad (2)$$

where, in the present case, r_d and r_m can be considered as the radii of nanoemulsion droplets and casein submicelles, respectively. The osmotic pressure can be calculated using a thermodynamic model, which assumes that all SC submicelles are spherical, and they exhibit uniform molecular weight

$$P_{osm} = nK_B T \left(1 + \frac{C_{aq}}{\rho} \right) \quad (3)$$

where n is the number density of the SC submicelles ($n = C_{aq} N_A / M$), C_{aq} the aqueous phase excess protein concentration, N_A the Avogadro number, M the effective molecular weight, and ρ the density of the sub-micelle particles ($\sim 1050 \text{ kg/m}^3$). $K_B T$ is the thermal energy of the system. The molecular weight of the SC submicelle was estimated as a function of its radius

$$M = \frac{4}{3} \pi r_m^3 \rho N_A \quad (4)$$

From Eqs. 3 and 4 it can be seen that the osmotic pressure and hence the depletion interaction energy is inversely proportional to the SC submicelle size and molecular mass. Therefore, the smaller the caseinate submicelle, the stronger will be the depletion attraction although the range of depletion interaction is directly proportional to the sub-micelle size. Taking the range of attraction in consideration Redford and Dickinson in

(2004) showed that the smallest depletant produced the strongest attraction, but they were very short-range where the attraction could be dominated by electrostatic or steric repulsion. On the other hand, larger sub-micelles, although produce weak depletion attraction, were long-range, and the overall interaction potential was dominated by attraction. In order to understand how SC submicelle size influence attraction when the droplet surfaces touch, we have calculated depletion interaction in terms of $K_B T$ for a range of sub-micelle size (5, 10 and 20 nm) (Fig. 6a) for the four nanoemulsions with increasing unadsorbed aqueous phase protein concentration (C_{aq}). The values of C_{aq} was calculated from the surface load analysis where NEs were ultracentrifuged to separate the cream layer from the serum layer and the protein concentration in the serum layer was determined by Dumas method (quantitative method to determine nitrogen content) (data not shown). It can be observed that depletion attraction increased with increase in un-adsorbed protein in the aqueous phase. This was also reflected by the visual observation and creaming index values for all NEs where the extent of creaming (driven by depletion flocculation) increased with increase in protein concentration. It should also be noted that the maximum attraction values fall within $2 K_B T$ for the smallest sub-micelles size (5 nm) indicating weak attraction among the droplets. Therefore, the flocs formed due to depletion are weak and will tend to break apart with a mere influence of thermal motion. This was reflected from the droplet size, creaming and visual observation results of all our NEs. As stated previously, the cream layer formed was so weak that a mere shaking of the vials containing NEs re-dispersed the flocs, thereby having no effect on the droplet size behaviour.

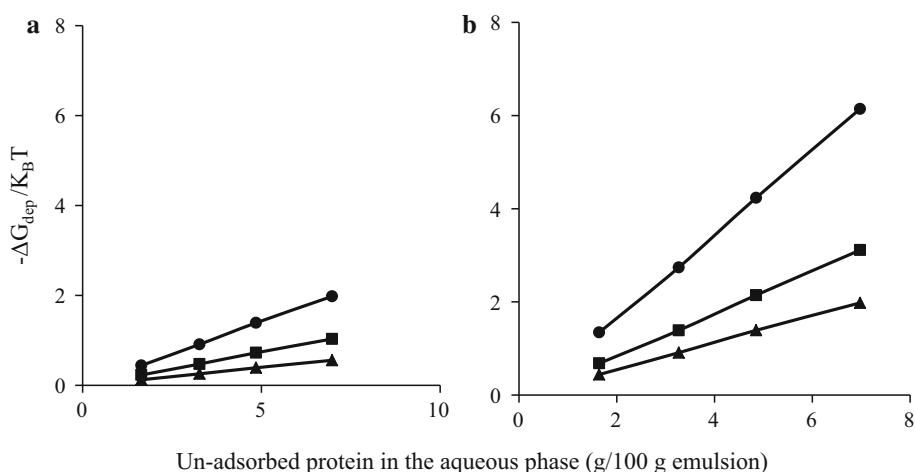


Fig. 6 Calculated values of depletion interaction energy ΔG_{dep} (units of $K_B T$) as a function of unadsorbed protein concentration in the aqueous phase of the nanoemulsions for (a) different caseinate submicelle radii: 5 nm (filled circle), 10 nm (filled square), 20 nm

(pointed up filled triangle) for 78 nm average droplet diameter of nanoemulsion, and (b) different average droplet radii: 500 nm (filled circle), 250 nm (filled square), 78 nm (pointed up filled triangle) for 10 nm caseinate submicelle

Nevertheless, for a sub-micelle size of 10 nm, reported by a vast majority of researchers (Liang et al. 2014) oil droplet size can also have a significant influence on depletion attraction. It can be seen from Fig. 6b that depletion attraction increased with increase in emulsion droplet size. For NEs with an average droplet radius ~ 78 nm (as in the present case) depletion attraction ranged from 0.4 to 1.9 times $K_B T$, while for a conventional emulsion with 500 nm droplet radius it varies from 1.3 to 6.4 times $K_B T$ with increase in protein concentration. This explain why our NEs even with high unabsorbed protein load showed very weak depletion attraction while conventional emulsions prepared by Liang et al. (Liang et al. 2014) (average droplet radius 365 nm) showed extensive depletion flocculation in the range of 1.0–15.6 times $K_B T$ for protein concentration of 1.5–10% wt%. This inherent advantage of NEs against depletion-induced destabilization makes them more suitable for applications where creaming stability is important.

Conclusion

Stable 5 wt% O/W NEs were developed with various concentrations of SC as sole emulsifier. All NEs remained stable to coalescence over the 6 months with no change in droplet size, although, excess un-adsorbed protein in the continuous phase induced reversible depletion flocculation and creaming of nanodroplets, which was confirmed by confocal microscopy. The nanodroplet flocs broke apart upon gentle mixing and had no effect on droplet size measurement using a static light scattering instrument. The formation of the cream layer from freshly made NEs was very rapid, and a discernable cream layer was visible within few hours after preparation. The thickness of the cream layer increased with increase in protein concentration and the full extent of creaming took about a week to form, thereafter compaction of cream layer began, which stopped when no more oil droplets and associated proteins can be packed.

Depletion interaction energy was quantitatively estimated using the theory proposed by Dickinson and co-workers (Dickinson et al. 1997). It was found that depletion attraction significantly reduced with decrease in droplet size. For the NEs considered in this work, with an average droplet radius ~ 80 nm, depletion attraction ranged from only 0.4 to 1.9 times $K_B T$ demonstrating inherent advantage of NEs against depletion induced destabilization. The knowledge developed from this work could be useful in understanding the effect of protein concentration on the long-term stability of NEs and can be applied in food and beverages as well as in pharmaceutical and cosmetics industries.

Acknowledgements Financial support for this work was provided by the Agriculture Development Fund (ADF) from Saskatchewan Ministry of Agriculture, CFI-John R. Evans Leaders Fund, Innovation and Science Fund (ISF) from Saskatchewan Ministry of Advanced Education and University of Saskatchewan New Faculty Start-up Equipment Support grant. We are grateful to Tara McIntosh and Suneru Ussetti Mohottalalage from the Protein research lab in Agriculture and Agri-food Canada, Saskatoon research center, for their help in nitrogen analysis. Helpful discussion with Dr. Michael Nickerson of Dept. of Food and Bioproduct Sciences and Dr. Janitha Wanasundara of Agriculture and Agri-food Canada are also acknowledged.

References

- Acosta E (2009) Bioavailability of nanoparticles in nutrient and nutraceutical delivery. *Curr Opin Colloid Interface Sci* 14:3–15
- Ahmed K, Li Y, McClements DJ, Xiao H (2012) Nanoemulsion-and emulsion-based delivery systems for curcumin: encapsulation and release properties. *Food Chem* 132:799–807
- Aleandri R, Schneider JC, Buttazzoni LG (1968) Evaluation of milk for cheese production based on milk characteristics and Formagraph measures. *J Dairy Sci* 72:1967–1975
- Aronson MP (1989) The role of free surfactant in destabilizing oil-in-water emulsions. *Langmuir* 5:494–501
- Detloff T, Sobisch T, Lerche D (2013) Instability index. *Dispers Lett Tech* T4:1–4
- Dickinson E, Golding M (1997) Depletion flocculation of emulsions containing unadsorbed sodium caseinate. *Food Hydrocoll* 11:13–18
- Dickinson E, Golding M, Povey MJ (1997) Creaming and flocculation of oil-in-water emulsions containing sodium caseinate. *J Colloid Interface Sci* 185:515–529
- Erramreddy VV, Ghosh S (2014) Influence of Emulsifier Concentration on Nanoemulsion Gelation. *Langmuir* 30:11062–11074
- Fernandez P, André V, Rieger J, Kühnle A (2004) Nano-emulsion formation by emulsion phase inversion *Colloid Surf, A* 251:53–58 doi:10.1016/j.colsurfa.2004.09.029
- Galooyak SS, Dabir B (2015) Three-factor response surface optimization of nano-emulsion formation using a microfluidizer. *J Food Sci Technol* 52:2558–2571
- Fillery-Travis AJ, Gunning PA, J. HD, Robins MM (1993) Coexistent phases in concentrated polydisperse emulsions flocculated by nonadsorbing polymer *J Colloid Interface Sci* 159:189–197
- Gutiérrez JM, González C, Maestro A, Solè I, Pey CM, Nolla J (2008) Nano-emulsions: New applications and optimization of their preparation *Curr Opin Colloid. Interface Sci* 13:245–251
- Hashtjin AM, Abbasi S (2015) Optimization of ultrasonic emulsification conditions for the production of orange peel essential oil nanoemulsions. *J Food Sci Technol* 52:2679–2689
- He W, Tan Y, Tian Z, Chen L, Hu F, Wu W (2011) Food protein-stabilized nanoemulsions as potential delivery systems for poorly water-soluble drugs: preparation, in vitro characterization, and pharmacokinetics in rats. *Int J Nanomed* 6:521–533
- Hunt JA, Dalglish DG (1994) Adsorption behaviour of whey protein isolate and caseinate in soya oil-in-water emulsions. *Food Hydrocoll* 8:175–187
- Karaca AC, Low NH, Nickerson MT (2011) Emulsifying properties of chickpea, faba bean, lentil and pea proteins produced by isoelectric precipitation and salt extraction. *Food Res Int* 44:2742–2750
- Lawrence MJ, Rees GD (2000) Microemulsion-based media as novel drug delivery systems. *Adv Drug Deliv Rev* 45:89–121
- Lee SJ, McClements DJ (2010) Fabrication of protein-stabilized nanoemulsions using a combined homogenization and amphiphilic solvent dissolution/evaporation approach. *Food Hydrocoll* 24:560–569

- Lee L, Norton IT (2013) Comparing droplet breakup for a high-pressure valve homogeniser and a microfluidizer for the potential production of food-grade nanoemulsions. *J Food Eng* 114:158–163
- Lerche D (2002) Dispersion stability and particle characterization by sedimentation kinetics in a centrifugal field. *J Dispers Sci Technol* 23:699–709
- Liang Y, Gillies G, Patel H, Matia-Merino L, Ye A, Golding M (2014) Physical stability, microstructure and rheology of sodium-caseinate-stabilized emulsions as influenced by protein concentration and non-adsorbing polysaccharides. *Food Hydrocoll* 36:245–255
- McClements DJ (1994) Ultrasonic determination of depletion flocculation in oil-in-water emulsions containing a non-ionic surfactant. *Colloid Surf A* 90:25–35
- McClements DJ (2005) *Food emulsions: principles, practices, and techniques*. CRC Press, New York
- McClements DJ (2007) Critical review of techniques and methodologies for characterization of emulsion stability. *Crit Rev Food Sci Nutr* 47:611–649
- McClements DJ (2011) Edible nanoemulsions: fabrication, properties, and functional performance. *Soft Matter* 7:2297–2316
- McClements DJ (2012) Nanoemulsions versus microemulsions: terminology, differences, and similarities. *Soft Matter* 8:1719–1729
- Newling B, Glover PM, Keddie JL, Lane DM, McDonald PJ (1997) Concentration profiles in creaming oil-in-water emulsion layers determined with stray field magnetic resonance imaging. *Langmuir* 13:3621–3626
- Paul D, Dey TK, Mukherjee S, Ghosh M, Dhar P (2014) Comparative prophylactic effects of α -eleostearic acid rich nano and conventional emulsions in induced diabetic rats. *J Food Sci Technol* 51:1724–1736
- Qian C, McClements DJ (2011) Formation of nanoemulsions stabilized by model food-grade emulsifiers using high-pressure homogenization: factors affecting particle size. *Food Hydrocoll* 25:1000–1008
- Radford SJ, Dickinson E (2004) Depletion flocculation of caseinate-stabilised emulsions: what is the optimum size of the non-adsorbed protein nano-particles? *Colloid Surf A* 238:71–81
- Rao J, McClements DJ (2012) Food-grade microemulsions and nanoemulsions: role of oil phase composition on formation and stability. *Food Hydrocoll* 29:326–334
- Sanguansri P, Augustin MA (2006) Nanoscale materials development – a food industry perspective. *Trend Food Sci Tech* 17:547–556
- SenGupta S, Ghosh M (2015) Formulation development and process parameter optimization of lipid nanoemulsions using an alginate-protein stabilizer. *J Food Sci Technol* 52:2544–2557
- Tadros T, Izquierdo P, Esquena J, Solans C (2004) Formation and stability of nano-emulsions. *Adv Colloid Interface Sci* 108:303–318
- Walstra P (2002) *Physical chemistry of foods*. CRC Press, New York
- Wooster TJ, Golding M, Sanguansri P (2008) Impact of oil type on nanoemulsion formation and ostwald ripening stability. *Langmuir* 24:12758–12765
- Xue J, Zhong Q (2014) Thyme oil nanoemulsions coemulsified by sodium caseinate and lecithin. *J Agric Food Chem* 62:9900–9907
- Zeeb B, Herz E, McClements DJ, Weiss J (2014) Impact of alcohols on the formation and stability of protein-stabilized nanoemulsions. *J Colloid Interface Sci* 433:196–203
- Zhao Q, Long Z, Kong J, Liu T, Sun-Waterhouse D, Zhao M (2015) Sodium caseinate/flaxseed gum interactions at oil–water interface: effect on protein adsorption and functions in oil-in-water emulsion. *Food Hydrocoll* 43:137–145. doi:10.1016/j.foodhyd.2014.05.009